CO_2 laser for lidar applications, producing two narrowly spaced independently wavelength-selectable *Q*-switched output pulses

Harley V. Piltingsrud

In this research directed toward using lidar methods for mapping concentrations of a variety of hazardous gases and vapors in an indoor workplace, a need was identified for a CO_2 laser that would meet certain special requirements, including an ability to produce 50–100-ns FWHM pulses in pulse pairs having interpulse spacings of 5–100 μs with each pulse of the pair being independently wavelength selectable. A laser was constructed with a low-pressure CO_2 amplifier section because of CO_2's long upper lasing level lifetime (>60 μs). This permitted the *Q* switching of two output pulses from a single laser amplifier electrical transverse discharge pulse, while allowing several microseconds for wavelength changing between pulses. An intracavity beam telescope was employed to use the amplifier discharge cavity cross section efficiently with the small CdTe *Q*-switch crystals available. A 1200-Hz oscillating grating with a high-resolution grating position sensor was used to change and reprogram wavelengths rapidly. Programming of wavelengths was accomplished by selecting appropriate delay times from the grating position reference signal for triggering the laser amplifier and the *Q* switch. Most of the basic performance goals of the device were achieved in the laboratory prototype.

Key words: CO_2 laser, *Q* switch, lidar.

I. Introduction

CO_2 lasers have commonly been used for differential absorption light detection and ranging (lidar) of chemical pollutants. The use of lidar methods for mapping concentrations of a wide variety of hazardous gases and vapors in an indoor workplace could substantially improve the ability to monitor and reduce exposure of employees to these substances. In pursuit of such technology, the need for a CO_2 laser with special requirements was identified. These requirements included a long service life; moderate costs; compactness; low mass; low power consumption; output pulses of an approximately Gaussian shape, with full width at half-maximum (FWHM) values adjustable from 50 to 100 ns; an ability to produce pulse pairs having interpulse spacings of 5–100 μs with each pulse of the pair being independently wavelength selectable; a repetition rate for the pulse pair of up to 10 Hz; a pulse energy of ~5–10 mJ; a tunable range covering most CO_2 laser emission lines; and pulse-pair wavelengths reprogrammable between pulse pairs.

These design goals resulted from a desire to use time of flight as part of the ranging method in the system. A narrow, nearly Gaussian pulse shape without tailing was pursued to permit a time-of-flight ranging resolution down to 10 m (achievement of additional range resolution is believed possible by combination with triangulation ranging) and to avoid using complex methods to reduce output-pulse tailing effects in the lidar return signals. The narrow temporal spacing between pulses in the pulse pair served to maximize atmospheric freezing, that is, ensuring that the atmospheric sample in the beam path did not change substantially during the time required to make a differential absorption measurement, even in environments having air velocities >100 m s^{-1}. This necessitated the use of a method to change the emission wavelength of the laser rapidly between the two pulses used in the differential measurement.

Previous investigators have reported on methods of rapid wavelength changing for CO_2 lasers using a rotating grating,[1] or similarly, a rotating mirror with a reflected grating,[2] and a galvanometer-movement rotated grating method.[3] In each of these cases a single output pulse was produced for each laser electrical

The author is with the National Institute for Occupational Safety and Health, 4676 Columbia Parkway, Cincinnati, Ohio 45226.
Received 6 April 1990.
0003-6935/91/273952-12$05.00/0.

discharge pulse, using a CO_2 transverse-excited atmospheric pressure (TEA) laser. The first system[1] relied on gratings mounted as a polygon structure at the end of the optical cavity with the polygon rotated at 105 rad s^{-1}. The TEA laser was fired when the grating position corresponded to the desired laser line, as sensed by an angular encoder. Wavelength rates of change of $\sim 1 \times 10^3$ $\mu m\, s^{-1}$ were produced. Faxvog and Mocker[1] also proposed an alternative application of this method that used a fixed grating with a rotating octagonal mirror reflecting the grating's image into the laser cavity. This method was implemented by Fox and Ahl,[2] where the mirror operated at angular velocities up to 314 rad s^{-1}, producing wavelength rates of change up to 6.7×10^3 $\mu m\ s^{-1}$. Fox and Ahl also applied a similar method to a Q-switched cw CO_2 laser for heterodyne detection applications, producing ~400-ns FWHM pulses with tailing.[3] The galvanometer driven grating method of Crocker[4] allowed the laser wavelength to be selected rapidly by applying a precisely controlled voltage to the galvanometer, producing a specific angular deflection of the grating corresponding to the laser line desired. Owing to inertial properties of the system, a maximum of 100 such wavelength selections could be accomplished each second. The galvanometer was capable of operation in an oscillating mode at frequencies up to 100 Hz, resulting in an average rate of wavelength change of 400 $\mu m\, s^{-1}$ when a full mechanical angular excursion of 8.6° was used. Increasing the angular excursion to the device's limits (25°) could increase this rate by a factor of ~1.5, assuming a sinusoidal angular velocity distribution for the grating's motion and that the wavelength range of interest was centered in the wavelength scan range. In most of the cases above, TEA lasers were used, which produced output pulses of ~100 ns FWHM with an output-pulse tail lasting up to a few microseconds. The rotating grating or mirror systems tended to eliminate some of the pulse-tailing effects of TEA lasers.[2] TEA lasers also were limited in their pulse repetition rates up to 300 Hz for commercial systems, with some producing up to 1000 Hz in short pulse-train bursts. Because of the normal pulse repetition limitations of available TEA lasers, the production of a second wavelength-shifted pulse would typically be within 10 ms, with the most rapid being within 1 ms. The higher pulse repetition rates were associated with relatively large and expensive lasers.

Some investigators have used two separate lasers fired in rapid sequence to produce two closely spaced pulses of different wavelengths; however, this may have disadvantages in cost, mass, size, rapidity of selecting new wavelengths, and accuracy of beam alignment compared with a single laser performing the same functions.

It became apparent that, if the desired pulse-pair separation were to be produced from a single laser, a method with a rapid wavelength-changing feature and either the capability of a long laser pulse or the ability of the laser to be re-pulsed rapidly would be required. The methods used by other workers appeared to have several shortcomings for this application. These shortcomings included the long pulse lengths or the low pulse repetition rates of the TEA lasers used as well as the poor longevity and dependability of wavelength-changing components under field conditions and, in some cases, the insufficient rapidity of wavelength changes.

II. Methods

A. Wavelength-Selection Mechanism

Selecting a pair of CO_2 laser emission lines between ~9.1 and 11.0 μm (a typical tuning range of CO_2 lasers) in a time interval <100 μs required for atmospheric freezing would require a wavelength rate of change averaging $\sim 1.9 \times 10^4$ $\mu m\, s^{-1}$, or with a 140-lines mm^{-1} grating, an angular velocity of 1.9×10^3 rad s^{-1}. A differential absorption lidar system must make a measurement on an absorption line for a chemical species of interest and a measurement off any absorption line for that species. Thus most applications for differential absorption measurements would require much smaller wavelength changes between the pulses of a pulse pair than the full range of the CO_2 laser spectrum. In this respect wavelength changes $\leq 1/10$ of the maximum tuning range of the CO_2 laser would be typical, requiring grating angular velocities of ~190 rad s^{-1}.

Resonant scanners were not mentioned in the literature surveyed for this application. A resonant scanner manufactured by General Scanning Corporation, Watertown, Massachusetts (Model IDS) is available for operation at higher frequencies than are the galvanometer types. Its basic performance specifications were quite similar to the General Scanning Model 325D galvanometer used by Crocker *et al.*,[4] which had a peak-to-peak wobble of 25 μrad and scan angular excursions of 25° (mechanical) but the IDS has a 1200-Hz operating frequency and a 10-mm-diameter mirror. The IDS resonant scanner also has much less sensitivity to external vibrations and temperature and a superior amplitude stability by a factor of ~10 over the Model 325D. The IDS also has a lower cost and a much longer life expectancy than the galvanometer system because it uses a rigid torsion bar suspension instead of ball bearings, which are highly sensitive to dust.

The maximum angular velocity of the 1200-Hz IDS was comparable with that of the rotating mirror system used by Fox and Ahl when it was operated at its maximum angular velocity of 314 rad s^{-1} (Refs. 2 and 3). However, the manufacturer's data show an expected lifetime for that scanner motor to be 5000–10,000 h. Vapors from motor bearing lubricants can also contaminate optical surfaces. Such devices appear to be less shock resistant than the resonant scanner and cost much more. For these reasons, the General Scanning Model IDS resonant scanner was selected for use in this study. A variation of the Model IDS scanner (Model Z2460) was also available, with a 19-mm-diameter mirror versus a 10-mm mirror for the IDS and operating at 1100 Hz.

Conversion of the oscillating mirror to an oscillating grating was accomplished by having the Milton Roy Company (Rochester, New York) place a grating replicate over the model IDS scanner mirror surface. This company could produce gratings blazed for a 26° 45′ angle at either 135 or 150 lines mm^{-1}. The manufacturer stated that the 150-lines mm^{-1} grating produced the highest tuning wavelength resolution; however, the grating's efficiency peaked for the 10P band at ~96% at 11 μm and at ~88% for the 9R band. The 135-lines mm^{-1} grating had similar peak efficiencies, but with the maximum close to 10.6 μm, and a higher efficiency remaining in the 9R band than did the 150-lines mm^{-1} grating. The higher tuning resolution 150-lines mm^{-1} grating was chosen for use in this study.

The Model IDS scanner with its Model AX730 driver provides a position timing signal for the mirror; however, the manufacturer specified its accuracy as only ±1.0%, and it was not sensitive enough to changes in scan angle amplitude. The use of this position reference was tried unsuccessfully, necessitating the design of a better position-indicating system. Consequently, a special electro-optical timing signal generator was designed and constructed (Fig. 1). This consisted of a 0.5-mW He–Ne laser projecting a beam onto a small mirror surface, A, located along the top edge of the grating. The beam was reflected off mirror B as a scan line, the ends of which were reflected by mirrors C and D to high-speed P-I-N photodiodes E and F. The timing signals produced by these photodiodes have

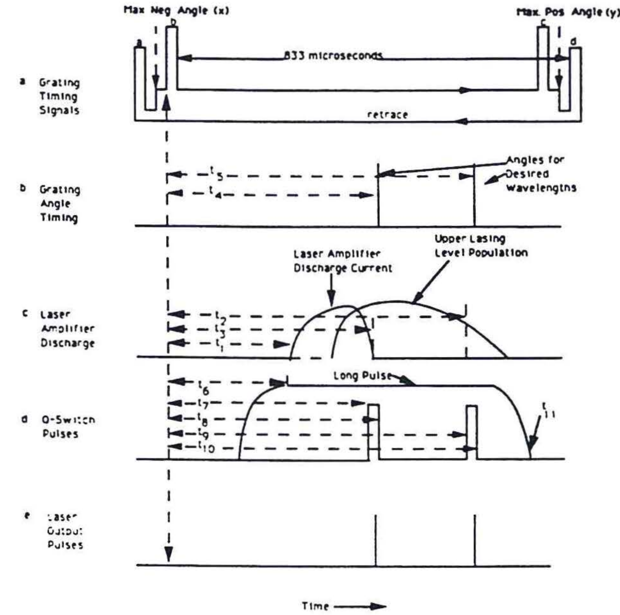

Fig. 2. CO_2 laser timing diagram.

temporal positions corresponding to the grating angular positions (Fig. 2). Figure 2 shows the temporal relationships of the output signals and the grating angle. Angles x–y are along the scan direction. Angles y–x are the retrace of the scan to the scan starting position. Photodiode E produces pulses a and b, corresponding to timing signals before and after the mirror reaches its maximum negative angle x. Similarly,

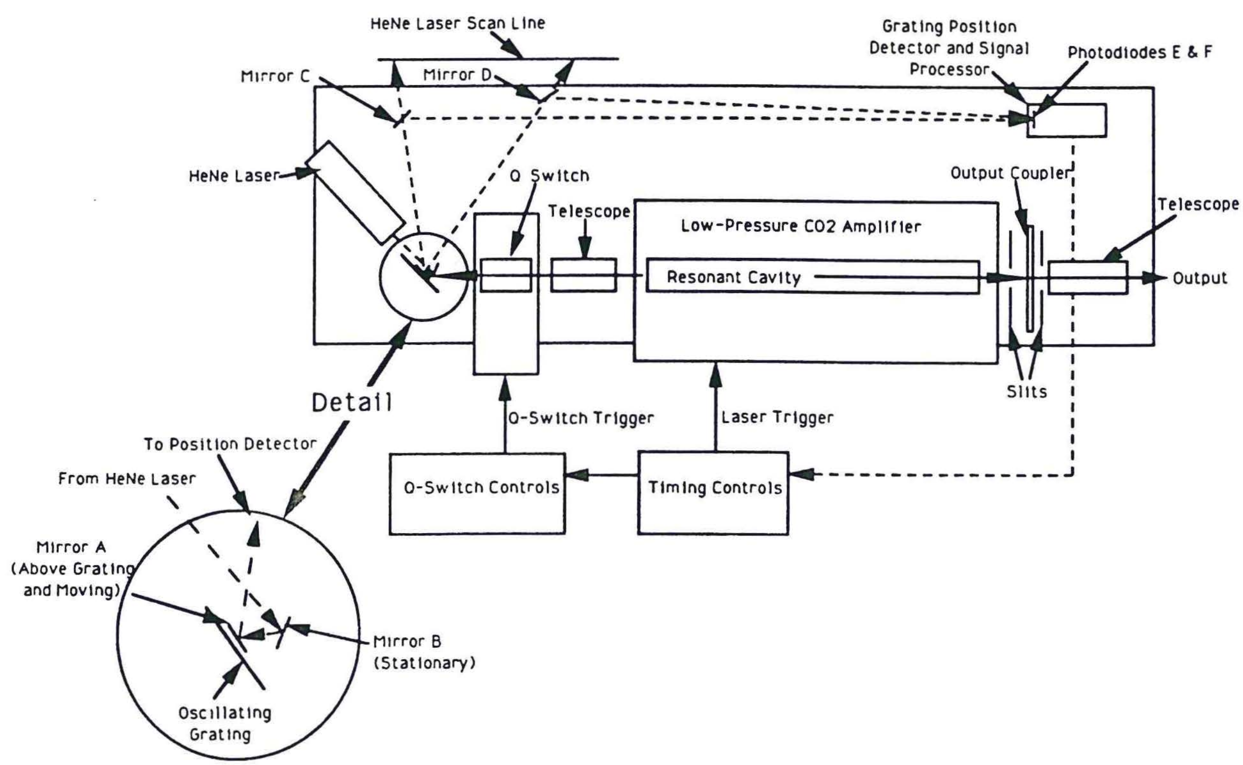

Fig. 1. Q-switched double-pulse CO_2 laser.

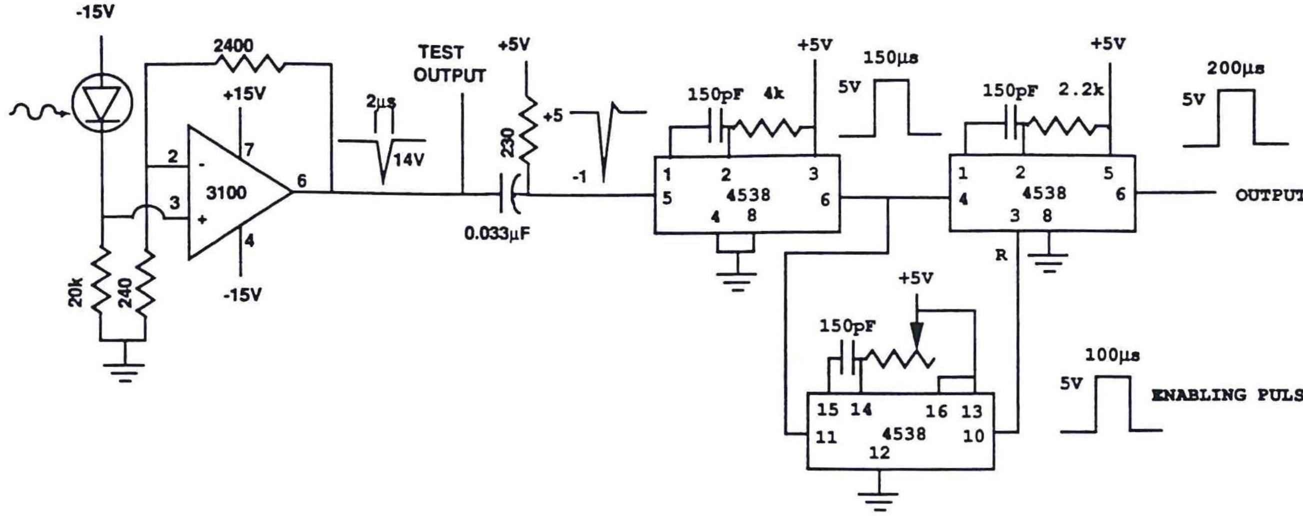

Fig. 3. Grating position sensing circuit.

photodiode F produces pulses c and d, corresponding to timing signals before and after the mirror reaches its maximum positive angle y. Logic circuits then produce a single timing pulse corresponding to the leading edge of pulses b and d only (see the electrical schematic, Fig. 3). Changes in the gratings' total scan angle are monitored by observing changes in the time interval between pulses b and d. The stability of the timing signals was observed by measuring the timing jitter between the leading edges of successive b output pulses and between b and d output pulses. This timing jitter could be a result of electrical noise, mechanical vibrations in the assembly, grating drive instabilities, etc.

B. Choice of a Laser

Some TEA lasers offer the advantage of achieving high output-pulse energies in a compact and lightweight assembly. However, it appeared that currently available TEA lasers were inadequate to produce the sequential pulses at the desired pulse spacing because of pulse tailing as well as pulse repetition rate limitations. Lower-pressure pulsed CO_2 lasers were also examined; however, problems similar to those of the TEA lasers existed. Q switching of CO_2 lasers was examined next. Q switching of low-pressure cw lasers offered the possibility of sequential switching of the laser, producing the desired pulse-pair spacing. Q-switched pulse rise times can be estimated[5] by calculating the pulse buildup time as follows:

$$n(t) = n_i e \exp(r - 1)t/\tau_c, \qquad (1)$$

where

$n(t)$ is the photon number at time t,

n_i is the initial photon number,

r is the ratio of inverted population n_i to threshold population n_{th},

τ_c is the cavity-inverted population lifetime (s),

t is the pulse buildup time (s), and

$\tau_c = 2d/c(1 - R)$,

where d is the cavity length (m),

R is the cavity loss factor, and

c is the velocity of light (m s^{-1}).

It can be seen that for rapid rise times in the Q-switched pulse, values of r should be large and d and R should be small. Unfortunately the values of r or R are not readily available for many lasers now available, particularly after Q-switch components have been added to their cavities. For most cw CO_2 lasers the value of r is rather small.[5] The resulting low-cavity gain and long pulse buildup time would be likely to pose a problem in meeting the performance goals. The low gain could be further aggravated by the addition of Q-switch-related optical components to the laser cavity. Manufacturers report Q-switched power levels for certain cw lasers of ~10 times the average power levels. If one assumed that this power level could be achieved with a suffucient pulse rise time and other necessary performance properties, the desired 10-mJ, 70-ns long pulses would require an ~700-W cw laser. In such a case pulse-pair repetition rates could be quite high, depending on the Q-switch performance specifications. A high average power cw laser did not seem the best candidate because of the low duty-factor requirements of the Q-switched system, as well as the low value of r, and because of the size, weight, cost, and poor pulse rise time of the laser.

Certain pulsed low-pressure CO_2 lasers offered some attractive features for this application relative to TEA lasers, including a longer discharge pulse and an increased CO_2 upper laser level population lifetime. This lifetime is dependent on both radiative and mechanical energy transfer mechanisms in the lasing medium. CO_2 upper laser level (00°1) spontaneous radiative lifetimes (under nonlasing conditions) (τ_2) are pressure dependent, ranging from 1 μs at a few hundred pascals to 3 μs at atmospheric pressure.[6] Another factor that could be important to an effective lifetime of the CO_2 upper lasing level is that the excited nitrogen level, $\nu = 1$, transfers energy rapidly[7] to various CO_2-excited energy levels ($00^\circ n$), which then decay with a characteristic lifetime ≈10 μs to the upper lasing level ($00^\circ 1$).[8] Thus an effective value for the upper lasing level population lifetime may be affected by other gases in the laser mixture that transfer some of their energy to the CO_2 ($00^\circ 1$) inverted population. It is also clear that the effective value for τ_2 is affected by many other factors specific to a given laser and certain operating conditions, including tube diameter, gas-flow rate, method of gas injection, current density, electron density, electron temperature, and gas temperature.[8] The short τ_2 for a TEA laser did not appear to allow sufficient time to change wavelengths and refire the Q switch of the laser. As discussed above, a second laser discharge pulse is generally not possible in <1 ms because of mechanical and chemical properties of the gas in the discharge tube. Thus this type of laser did not appear suitable for the proposed application.

Low-pressure transverse-excited CO_2 lasers having much longer discharge times (up to 300 μs) are available.[9] The τ_2 at a pressure of 6.7×10^3 Pa is greater than 50 μs, thus permitting sufficient time between Q-switched output pulses for substantial wavelength changes to occur.

After consideration of the ability of various lasers to be adapted to this application (including removable cavity end mirrors), only a few lasers remained to be considered. The laser amplifier section selected for further evaluation was a Model LP30 low-pressure transverse excited CO_2 laser manufactured by Pulse Systems, Inc., Los Alamos, New Mexico. The LP30 appeared to satisfy many of the requirements of this application, including low cost, low weight, compact size, low radio-frequency interference (RFI) generation, long lifetime, and range of operating pressure. Based on the manufacturer's recommendations as to how to achieve the best value of r, the shortest discharge time option for the laser was selected (~10 μs). The basic LP30 has dimensions of 10.5 cm × 21 cm × 50 cm and a mass of ~10 kg, including the laser discharge tube and power supplies. This laser amplifier is a gas-flow type (100 cc/min at 8×10^3 Pa operating pressure) with a preferred gas mixture of 15% N_2, 20% CO_2, and 65% He and a projected lifetime of $>10^8$ discharge pulses. The gas flow made necessary the use of a vacuum pump with the laser amplifier. A compact, low-mass (8-kg) long-lived rotary vane compressor (Whirlpool Corporation, Benton Harbor, Michigan Model 463926) was adapted to this use. When the LP30 is used in a simple non-Q-switched laser cavity, the manufacturer claims it can produce output energies up to 120 mJ/pulse on the 10P20 line. Laser operating pressures were measured with a capacitance manometer Model 122AA-00100AB with Model PDK-D-11 readout, manufactured by MKS Instruments, Inc., Andover, Massachusetts. The laser was constructed with all-optical cavity components and the grating position detection system mounted on a 2.5-cm-thick cast aluminum machined plate (ALCOA Alca Plus, Aluminum Company of America, Pittsburgh, Pennsylvania) as in Fig. 1. A Model PRZ 1.0-80-0000 80% reflectivity output coupler was used, manufactured by Laser Power Optics, San Diego, California.

C. Q Switch

The Q-switch assembly consisted of a CdTe electro-optical crystal (Pockels cell) and a high-voltage pulser. The sizes of the available crystals dictated many features of the assembly's design. The Pockels cell chosen was a CdTe model EQS5-10.0-0950-C crystal, manufactured by II-VI, Inc., Saxonburg, Pennsylvania, and, based on manufacturing constraints, was 9 mm × 9 mm × 50 mm in size.

All surfaces were polished, and the entrance and exit ends (9 mm × 9 mm) were antireflection (AR) broadband coated, with a bandpass centered at 10.0 μm. Minimum transmission, 9–11 μm, was 98.0%, with transmission 9.5–10.5 μm greater than 99.0%. The 1/4-wave polarization rotational voltage for this crystal was approximately 4500 V, which was well under the maximum allowed applied voltage of 10 kV recommended by the manufacturer, thus helping to ensure a long lifetime for the cell.

The laser discharge cavity had a cross section of 20 mm × 20 mm, which was substantially larger than the entrance window of the Pockels cell. To use the discharge cavity's cross section efficiently, an intracavity beam telescope was used (see Fig. 1). The telescope had a 3× magnification and was of a Galilean design, using ZnSe optics with broadband AR coatings having a bandpass centered at 10.0 μm. Transmission 9–11 μm was 98.0%, and transmission 9.5–10.5 μm was greater than 99.0%. It was manufactured by II-VI, Inc., Saxonburg, Pennsylvania as Model BECZ-10.0-C1.0:5-D3F.

The Q-switch electrical pulser was a modified version of one custom designed and manufactured by Letzring Associates, Honeoye Falls, New York. It was designed to provide two variably spaced (1–100-μs) output pulses, each having an independently preselectable pulse width from 20 to 1000 ns. The pulser was designed such that the two terminals of the Pockels cell normally are held at a common high potential almost equal to the desired 1/4-wave voltage for the cell (see Fig. 4). At time t_6 (see Fig. 2d), several microseconds before the laser discharge, the 1/4-wave voltage was applied across the Pockels cell by allowing tube T2 to conduct (T2 was an 8533-W medium-speed high-voltage triode). This caused the laser cavity Q to become low, preventing lasing. After an appropriate time interval for a selected grating position to be reached, at time t_7 [a short time before time t_4 (see Figs. 2b and 2d)] tube T1 (a Y690 high-current high-frequency microwave triode, chosen to provide rapid Q switching when lasing was to be initiated and terminated) was caused to conduct, bringing both terminals of the Pockels cell near a common ground potential. This created a high-laser cavity Q and caused lasing to build up in the cavity. To terminate lasing at time t_8, tube T1 conductance was stopped, returning the cavity to a low-Q condition. At time t_9, T1 was turned on and

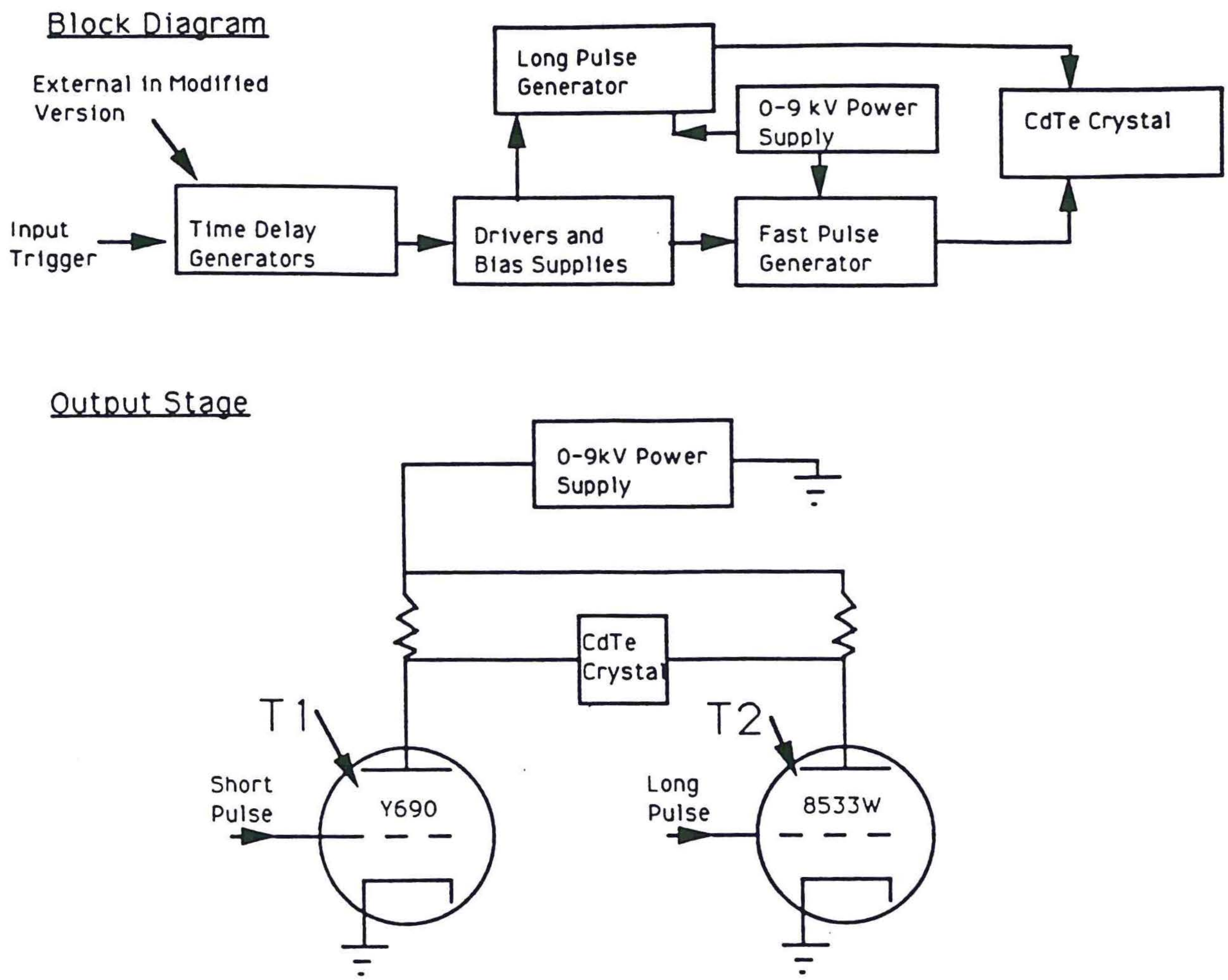

Fig. 4. *Q*-switch electrical pulse generator.

then off again at time t_{10} to allow for the second *Q*-switched output pulse associated with one laser discharge pulse. Times t_7 and t_9 precede times t_4 and t_5, respectively, to allow time for the laser pulse to build up in the optical cavity (this may require several hundred nanoseconds). Rise and fall time constants (to $^1/_{10}$ values) for the high-voltage switching pulse across the Pockels cell were ~8 and ~15 ns, respectively. These were measured with a high-frequency high-voltage probe, Model P6015 manufactured by Tektronix, Inc., Redland, Oregon. The turn-off time was perhaps the most important, because it defined the trailing edge of the laser *Q*-switched output pulse. The leading edge was most affected by the laser cavity lifetime (τ_c). Both of the high-voltage triodes used were operated well below their maximum voltage and current ratings. The maximum pulse repetition rate of the pulser was 30 Hz. As a result of erratic delay times in the unit supplied, a new delay time generator was constructed and located outside the pulser housing. This eliminated the problem.

The laser was environmentally stabilized by placing it in a closed housing with a recirculating air system. The air was passed through high-efficiency particulate and activated charcoal air filters and through a heater to stabilize the laser housing temperature at 38° ± 1°C by using a thermistor temperature sensor in the return air duct and a zero-crossover proportional heater power regulator (Model 72A, Dowty Electronics Company, Brandon, Vermont).

D. Measurements of the Laser's Performance

In practice, the production of two sequential *Q*-switched output pulses using one transverse discharge pulse requires a somewhat careful selection of operating parameters to maintain an adequate output energy for both pulses. It appeared likely that the relative intensity of the two output pulses would depend primarily on the time interval between the laser amplifier transverse discharge pulse and the first *Q*-switched pulse ($t_7 - t_1$) as well as on the pulse width of the first pulse ($t_8 - t_7$) (see Fig. 2). This involved ensuring that a sufficient population inversion ratio existed for the second pulse. Selecting a small time interval (5–15 μs) between the discharge pulse and the first *Q*-switched pulse should have resulted in an incomplete transfer of energy from the (00°*n*) CO_2-excited energy levels to the CO_2 (00°1) upper lasing level, as could be expected from the ~10-μs time constant for these transitions. Thus by the choice of an appropriate delay time, some energy still in the ($00^\circ n$) levels would be transferred to the ($00^\circ 1$) level after the first Q-switched pulse, helping to provide a sufficient population inversion ratio for the second pulse. Also, the choice of a narrow pulse width for the first pulse permits a significant population inversion ratio to remain for the second pulse. This would be due to the likelihood that a longer lasing time would be required for reducing the population inversion ratio during the first pulse to a level less than that required for significant lasing on the second pulse. Time intervals to the second pulse were also considered, as the lifetime of the CO_2 ($00^\circ 1$) level dictated the decay of the inversion ratio existing after the first pulse [see Eq. (1)].

Owing to the uncertainty surrounding an effective value for τ_2 for this laser assembly, measurements were made to evaluate the laser's ability to produce Q-switched output pulses as a function of time ($t_7 - t_1$) after the initiation of the laser transverse discharge pulse (see Fig. 2d). These measurements were taken using an 800-ns-wide electrical pulse on the Q switch, which resulted in an ~100 ns FWHM Q-switched output pulse. Laser gas pressures used were 5.3×10^3, 6.7×10^3, 8.0×10^3, and 9.3×10^3 Pa.

Measurements were made to examine the effects of the delay time to the first pulse ($t_7 - t_1$) on the output energy ratio of the first pulse to the second pulse. This was done for two sets of selected output emission line pulse pairs, 9P14 and 10R20, and 10P20 and 10P26. Delay times ($t_7 - t_1$) ranged from 6 to 22 μs. Measurements of both output pulse's energies were made with the first and second pulses each alone and with both produced together. The influence of pulse 1 on pulse 2 was seen by subtracting the energy of pulse 1 from the sum of pulses 1 and 2, yielding the value for pulse 2. These measurements were conducted using a laser gas pressure of 8.6×10^3 Pa and Q-switch electrical pulse widths of 660 and 800 ns for pulses 1 and 2, respectively.

Measurements demonstrating the effect of the first output pulse's width on the second output pulse's energy were made at emission lines 10P20 and 10P26 for pulses 1 and 2, respectively. These measurements were conducted at a laser gas pressure of 8.6×10^3 Pa and Q-switch electrical pulse widths of 660 and 800 ns for pulses 1 and 2, respectively, producing output pulse widths of ~70 ns FWHM.

Measurements were made that demonstrated the resolution of the tuning of the laser output wavelength over two groups of three emission lines, 9P12–9P16, and 10P18–10P22. Laser wavelength measurements were made with the CO_2 laser spectrum analyzer manufactured by Lasercraft, Inc., Optical Engineering Division, Santa Rosa, California. It was modified to lower the device's internal ultraviolet illumination of its fluorescent sensor screen so that laser output power levels of a few watts created visible lines on the spectrum analyzer screen. The laser output passed through a ZnSe telescope, reducing the beam waist to 3–4 mm, with near parallelism at the entrance to the analyzer, thus ensuring that most beam power was delivered to the analyzer. This was accomplished by using the CO_2 laser spectrum analyzer with the optional slit installed in the sensing screen position at the proper position for each laser line measured. A Calorimetrics, Inc. (Boulder, Colorado) Model TC 1 power meter detector was placed behind the slit to measure relative power passing through the slit. The wavelength interval was then scanned, using appropriate Q-switch time delays (t_7), and power versus wavelength was plotted for the three slit positions corresponding to the three output lines measured.

The pulse output energies of the laser are dependent on many factors, including the laser emission line selected, the spectral resolution of the laser (related to the cavity slit widths selected), the laser amplifier electrical discharge voltage and current, the laser amplifier gas pressure, the Q-switch electrical pulse width, and the relationship of the timing of the first and second pulse to that of the laser amplifier discharge. The choice of many of these operating parameters will depend on the application. When emission lines in the 9R and 9P emission bands were selected, narrower slit widths were normally selected because of the narrower line spacings. This resulted in a higher tuning resolution that eliminated the possibility of output on an adjacent line when the laser was properly tuned. When emission lines in the 10R and 10P bands were used, a wider slit was acceptable because of wider line spacings. Measurements were made of the energy output of the laser at CO_2 laser wavelengths, where a significant output (>1 mJ) existed, using a laser pressure of 8.6×10^3 Pa, a Q-switch electrical pulse width selected to produce an ~70 ns FWHM laser output pulse width, and laser settings selected for a higher tuning resolution (using 10-mm slits). The electrical discharge voltage for the laser amplifier (which was directly related to the gain of the amplifier) was selected for stable operation with a low incidence of arcs in the discharge, as well as a long life for the discharge tube, although operation with up to 50% greater pulse energy was possible.

The laser output pulse-to-pulse energy variations were measured for the 9R20 and 10P20 lines independently as well as the 10P20 line as a second output pulse following a 10P14 line pulse (pulse heights of each being approximately equal). These were measured with a liquid-nitrogen-cooled HgCdTe photovoltaic detector having rise and fall times (to $1/10$ values) of ~65 and ~160 ns, respectively. The somewhat poor high-frequency response of this detector was advantageous for this study because it integrated any higher-frequency structure of the laser output pulse, allowing the maximum peak height of the detector output to be almost directly proportional to the laser output pulse power. The detector viewed the reflection of the laser output beam from a diffusively reflective surface. For each of the 3 groups of measurements, 100 samples were taken at approximately equal time intervals over a period of 5 min.

Measurements of the laser output pulse shapes were made with a high-speed thermoelectric-cooled HgCdTe detector, Model J15TE4:10-MC31G-S01M with a Model TC-4 controller, both manufactured by Judson Infrared, Inc., Montgomery, Pennsylvania. The detector had a 1-mm-diameter detector element with an AR-coated germanium window. Its $1/e$ rise and fall times were <10 ns. This detector was used in conjunction with a Model CLC100 low-noise, wide-bandpass amplifier manufactured by Comlinear Corporation, Loveland, Colorado. A Model 54201A oscilloscope manufactured by Hewlett Packard Company, Palo Alto, California, was used to display and measure laser pulse shapes and widths. Measurements were made with the laser beam reflected off a diffuse reflecting surface and with the detector located 1 m from that surface.

E. Measurement Error

1. *Optical Power Measurements*

Measurements made with the Calorimetrics power meter had several sources of error. The basic long-term stability of the instrument was less than ±0.1% (1.0 s); however, measurements in the lower range of the instrument had a digital uncertainty of 0.1 mW. This contributed a maximum error of ±3.0% under the measurement circumstances in which the instrument was used. An uncertainty in the absolute calibration of the instrument at 10.6 μm may have contributed a measurement bias of up to 4.0%. If the digital error was considered to be random, then the maximum total random error of the measurement system was approximately ±3.0% (1.0 σ). Another, more difficult, source of error to evaluate was that due to the variation in the laser's pulse-to-pulse energy during the time that a measurement of optical power was made. It is estimated that this contributed less than ±4.0% (1.0 σ) of random error to the measurement. Thus the total random error is estimated to be less than ±5.0% (1.0 σ).

2. *Wave-form Measurements*

Timing measurements made with the Hewlett-Packard oscilloscope are specified by the manufacturer to have errors of less than ±2 ns or ±0.2% of the range selected, whichever was greater. In all cases, this source of error appeared to be negligible compared with operator interpretation errors in evaluating pulse width, time jitter, voltage, and current measurements. Operator interpretations probably added a random error of up to ±5.0% (1.0 σ). Voltage calibration biases for the oscilloscope were cited to be ±4.0%. Again, operator interpretations may have contributed a random error to these measurements of up to ±5.0% (1.0 σ). High-voltage measurements had an additional calibration bias of ±3.0%; thus a total measurement bias of ±7.0% was possible but unlikely. The laser discharge current measurements had possible biases of ±2.0% in addition to the voltage calibration bias and a random error similar to that of the voltage measurements.

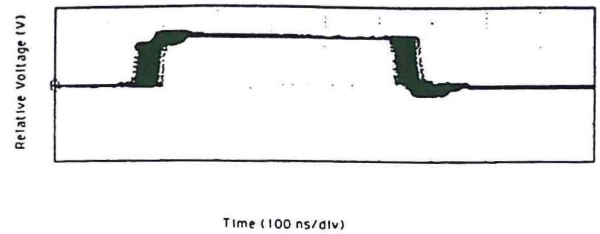

Fig. 5. Grating position sensor pulses b–d timing jitter for 120-s measurement.

III. Data and Discussion

Figure 5 shows the random timing variations (jitter) measured between the grating position signals b and d (see Fig. 2a). This timing jitter had maximum peak-to-peak variations of ~50 ns, measured over a time period of 2 min. This would correspond to an average angular error of ~0.0015° when a 25° mechanical scan angle is used, corresponding to an ~7.0×10^{-4}-μm wavelength range at the 10P20 emission line. Because the short-term amplitude and frequency stability of the resonant scanner are probably negligible, any short-term variations in the time between pulses b and d were assumed to be due to the instability of the grating position measurement system. Long-term stability of the overall wavelength tuning system was such that, after an initial warm-up of the system, a tuned pair of laser lines would normally stay tuned for at least 24 hs.

Figures 6 and 7 show the long and short electrical pulses applied to the Q-switch crystal and the typical output pulses from the laser (Figs. 8 and 9). Output-pulse widths (FWHM) typically varied less than +10% (1 σ) pulse to pulse. Measurements were made on the 10P20 line with a laser pressure of 8.6×10^3 Pa. It can be seen that, as the output pulse width is increased, increased evidence of modal beating appears in the fine structure of the pulse. Figure 10 shows a typical

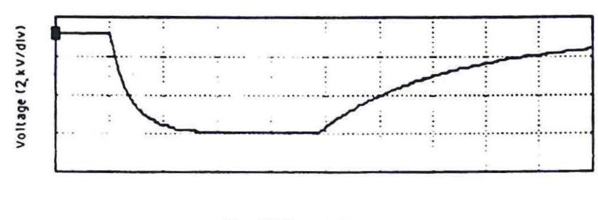

Fig. 6. Q-switch long-pulse.

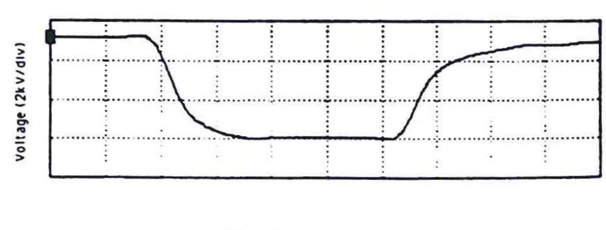

Fig. 7. Electrical pulse on a Q-switch crystal.

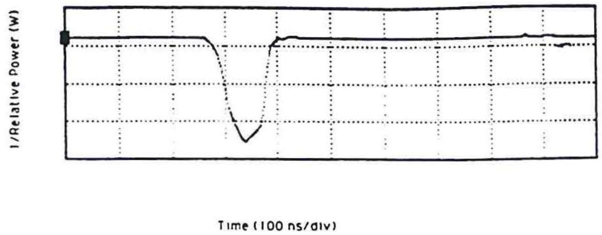

Fig. 8. Q-switched laser output pulse (~60 ns FWHM).

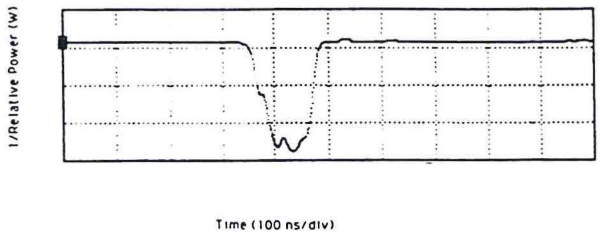

Fig. 9. Q-switched laser output pulse (~100 ns FWHM).

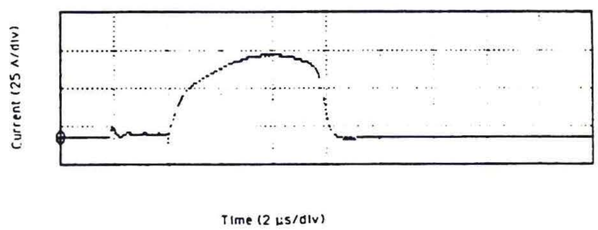

Fig. 10. Laser amplifier transverse electrical discharge pulse current.

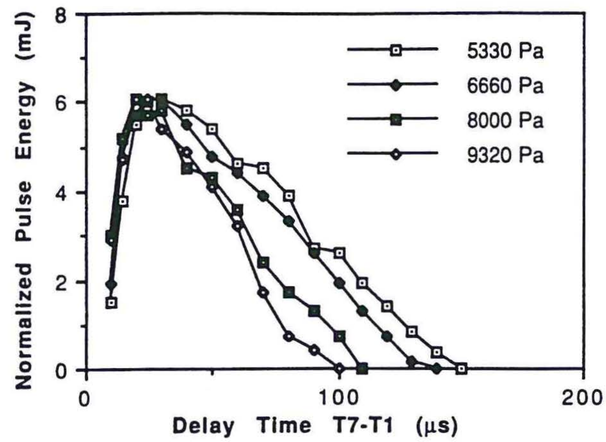

Fig. 11. Pulse energy versus pressure and delay time.

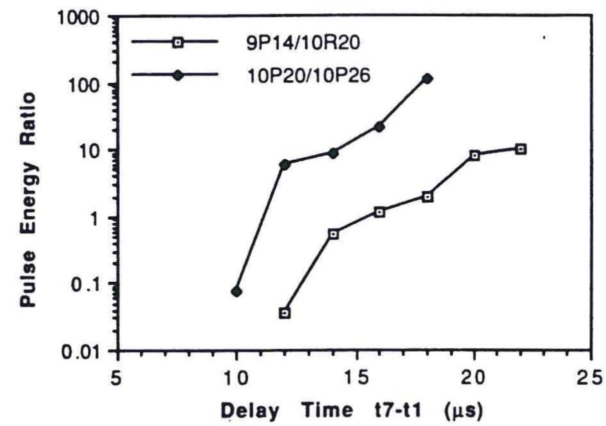

Fig. 12. Effect of delay $T_7 - T_1$ on ratio of output pulse energies.

laser amplifier transverse electrical discharge current pulse at an operating pressure of 8.6×10^3 Pa.

Figure 11 shows the laser output-pulse energy for the 10P20 line versus the time delay $(t_7 - t_1)$. The graphs are normalized to the highest pulse energy output data set (9.3×10^3 Pa). The laser discharge peak current was held constant during these measurements; however, there was a small change in the discharge current waveform as operating pressure changed, with an increased peaking toward the end of the pulse as the pressure increased. The data indicate that, under these conditions of operation, the maximum output of the laser occurs with a time delay $(t_7 - t_1)$ of ~20 μs, or ~10 μs after the laser current discharge had ceased. This was probably related to the time required for the decay of the CO_2 (00°n) states to the (00°1) state. The decay of the inverted population then decreases, with measurable lasing ceasing at $t_7 - t_1$ times ranging from ~95 μs at 9.3×10^3 Pa to ~140 μs at 5.3–9.3 $\times 10^3$ Pa. Greater than 50% of the maximum output energy remains at 60 μs for even the highest pressure used.

Figure 12 shows the effect of the delay time $t_7 - t_1$ on the output energy of a second pulse, spaced at 3.5 μs (10P20 and 10P26) and 49 μs (9P14 and 10R20) from the first pulse. It can be seen that the delay time at which lasing starts for the 10P26 emission line was 8 μs, as opposed to 12 μs for the 10R20 line. This is probably related to a higher cavity gain existing under such measurement conditions for the 10P26 line. It can be seen that, for both pulse pairs, the first pulse rapidly increases in energy as the delay time increases, out to ~18 μs. At delay times between the start of lasing for the first pulse and 18 μs, the energy of the first pulse increases until the remaining inversion ratio is inadequate for lasing on the second pulse. Figure 13 shows that an increasing Q-switch pulse width and consequent pulse energy for the first pulse (10P20 line) also affects the inversion ratio remaining for lasing on the second pulse (10P26 line). Figure 14 shows the correlation between Q-switch pulse width and laser output pulse width. The energy of the first pulse increased with increasing pulse width, with a minimum laser output pulse width of ~25 ns and a saturation of output energy at ~100 ns. The ratio of the energy of the first to the second pulse was approximately unity at a laser output pulse width of 50 ns, with an insufficient inversion ratio remaining for lasing in the second pulse when the first pulse width was >100 ns.

Figures 15 and 16 show the relative laser output versus relative delay time t_7 (relative grating wavelength position) for two sets of three sequential laser emission lines, 9P12, 9P14, and 9P16 and 10P18, 10P20, and 10P22. Because the output on the lines is measured separately, one can see the relative contribu-

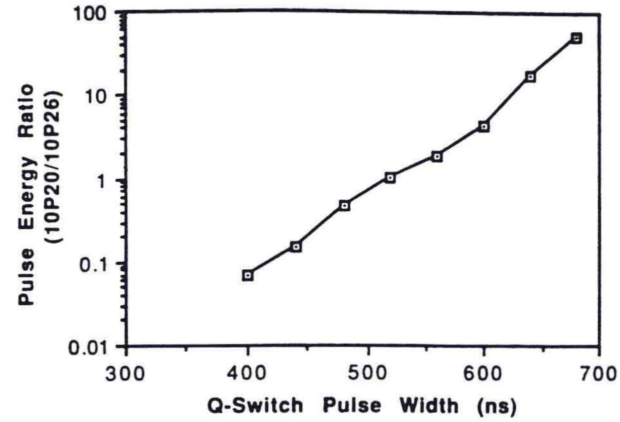

Fig. 13. Effect of Q-switch pulse width on ratio of first to second laser output-pulse energies.

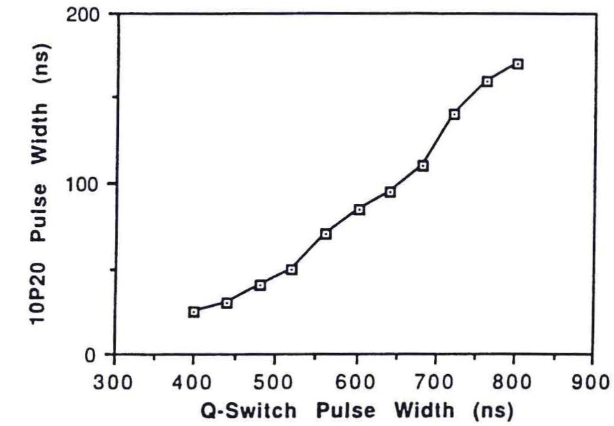

Fig. 14. Change in output-pulse width with Q-switch pulse width.

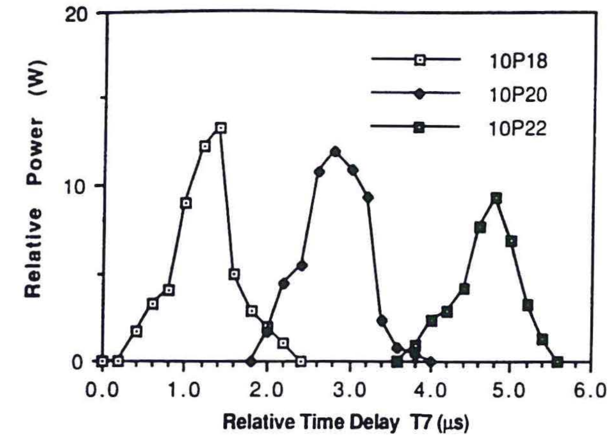

Fig. 15. Tuning of 10P20 emission line.

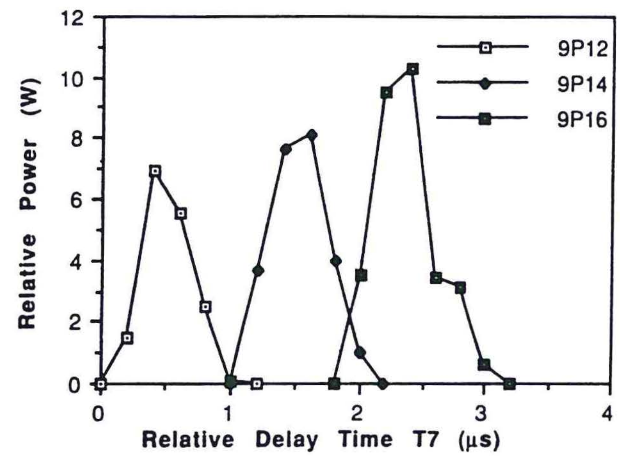

Fig. 16. Tuning of 9P14 emission line.

tion to the total output energy of each line, depending on the setting of t_7. In each line a proper choice of t_7 should yield a single line output for the laser. It can be seen from Figs. 15 and 16 that T7 time delay intervals between successive emission lines range from 1 to 2 μs, with peak tuning intervals of a few hundred nanoseconds. Thus the observed 50-ns tuning jitter does not appear to have a significant effect on the laser's tuning stability.

Figure 17 shows the laser output pulse energies versus output wavelengths for laser lines over the CO_2 laser spectrum. As a result of the reduced gain setting of the laser amplifier used for these measurements, many possible emission lines from the CO_2 laser spectrum were not present. This was particularly the case for the 9P emission band, because of the reduced grating efficiency in that wavelength region.

The measurements of the laser's output pulse-to-pulse energy variations for the 9R20 and 10P20 emission lines, individually, and the 10P20 line pulse preceded by a 10P14 line pulse, resulted in estimates of σ of 11.5%, 8.8%, and 21% of the mean values, respectively. The sources of these pulse-to-pulse variations are not known but were probably related to variations in the cavity Q resulting from the grating position, variations in r [see Eq. (1)], etc. The variations in output-pulse energy observed would result in most pulses' being acceptable for use in a differential absorption lidar system, where the outgoing energy of each pulse was measured and the return signals normalized accordingly.

Operating experience with the LP30 amplifier revealed that a significant fraction of transverse discharge pulses result in irregular current pulses with arcing in the gas discharge. This was accompanied by a cracking sound. The irregular pulses usually occurred in clusters. This problem can be minimized by long warm-up periods, lower discharge voltages and currents, better choice of operating pressure, etc. After an extensive search for a workable combination of operating parameters consistent with the desired laser outputs, the resulting percentage of irregular discharge pulses was <3.0%. Such pulses were eliminated from data collection by an audible monitoring of the laser. The use of a higher-gain laser amplifier having fewer arcing problems would substantially increase the number of emission lines that could be produced with stable operating conditions. This could be accomplished with the same type of low-pressure laser amplifier used in this study by using a longer discharge tube or tandem discharge tubes. Also, the laser amplifier manufacturer claims to have recently developed im-

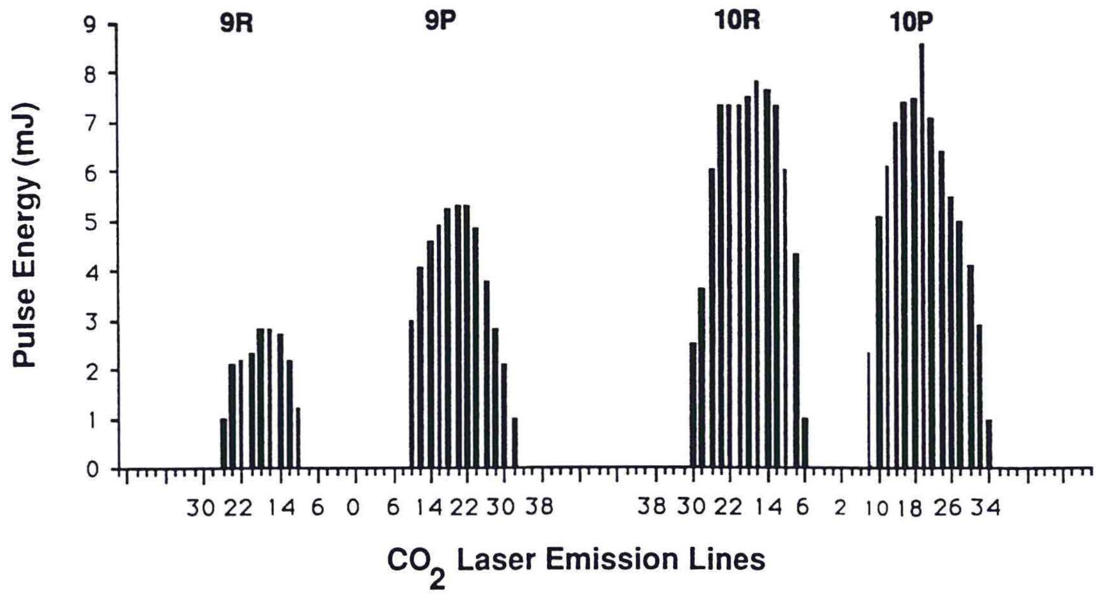

Fig. 17. Laser output-pulse energies.

provements for the amplifier used in this study by using voltage stabilization, discharge current regulation, and arc suppression circuits in its power supply. A sealed discharge tube laser amplifier having similar performance properties and physical characteristics would be desirable. This would eliminate the need for a lasing gas supply and a vacuum pump. The choice of a different grating having its peak efficiency closer to 10 μm would provide a more balanced cavity gain from 9.1 to 11 μm.

The initial alignment of the optical cavity involved the setting of the intracavity telescope focus. It should be mentioned that care should be taken to avoid a setting significantly different from parallel ray output for parallel ray input. Significant convergence in the output can result in high energy densities in the cavity, which could damage optical surfaces.

A retrospective examination of the laser cavity design for an enhanced longevity of optical components and a lower cavity loss has resulted in the consideration of alternative specifications for some components. These included the elimination of the intracavity telescope, use of the General Scanning Model Z2460 resonant scanner, which would permit a 19-mm diameter grating, and a change in the dimensions of the CdTe Q-switch crystal to one with dimensions of 10 mm × 16 mm × 35 mm. The 35-mm dimension would be along the optical axes of the cavity, and the 16-mm dimension would be parallel to the rotational axes of the grating. The Q-switch pulser high voltage would be increased to ~7600 V to accommodate the shorter crystal length. This design should lower the irradiance on all cavity optical components and provide a lower cavity absorption loss. A higher reflectivity output coupler (to >90%) should enhance lasing on weaker intensity lines. Piezoelectric transducer cavity length stabilization could also improve the pulse reproducibility of the laser. This would require the development of a fast, high-current driver for the piezoelectric elements.

The prototype's mass was ~50 kg, and its dimensions were ~30 cm × 120 cm × 20 cm. A separate housing for the Q-switch pulser power supply and controls was ~7 kg and had dimensions of approximately 53 cm × 50 cm × 22 cm. The housing for the laser was made of a heavy-gauge steel, chosen mostly for economy. The laser's mass could be substantially reduced by fabricating a lighter housing and reducing the mass of the aluminum plate on which the optical components were mounted. The Q-switch power supply and controls could be redesigned to fit into the existing laser housing with little added mass and with some reduction in RFI from its connecting cables.

IV. Conclusions

The laser prototype constructed appeared to meet most of the goals initially set for it. The laser amplifier evaluated has the potential for satisfying the long-life, moderate-cost, compactness, and low-mass goals. Other components, including the oscillating grating and Q-switch components, also met these goals. The system produced the desired pulse width, pulse shape, and wavelength-changing goals. The pulse output energy criteria were met for a large number of emission lines. Achieving some goals, such as a low mass and small size for the complete system and an improvement in the number of usable emission lines, appears to be an attainable objective for the next generation of the device.

The prototype laser system is now being used for laboratory studies of transmitter and receiver systems for an indoor differential absorption lidar system.[10]

References

1. F. R. Faxvog and H. W. Mocker, "Rapidly Tunable CO_2-TEA Laser," Appl. Opt. 21, 3986–3987 (1982).

2. J. Fox and J. Ahl, "High Speed Tuning Mechanism for CO_2 Lidar Systems," Appl. Opt. **25**, 3830–3834 (1986).
3. J. Fox and J. Ahl, "Tuning Device for CO_2 Hetrodyne Detection Lidar," Rev. Sci. Instrum. **60**, 1258–1261 (1989).
4. A. Crocker, R. M. Jenkins, and M. Johnson, "A Frequency Agile, Sealed-Off CO_2 TEA Laser," J. Phys. E **18**, 133–135 (1985).
5. A. Siegman, *Lasers* (University Science, Mill Valley, Calif. 1986).
6. A. Yariv, *Quantum Electronics* (Wiley, New York, 1975).
7. D. A. Eastham, *Atomic Physics of Lasers* (Taylor & Francis, London, 1986).
8. C. S. Willett, *Introduction to Gas Lasers: Population Inversion Mechanism* (Pergamon, New York, 1974).
9. Lasers and Optronics, *1989 Buying Guide* (Gordon, Dover, N.J., 1989), pp. 164–180.
10. H. V. Piltingsrud, "Tunable CO_2 laser-based photo-optical systems for surveillance of indoor workplace pollutants," in *Proceedings of the Second International Symposium on Field Screening Methods for Hazardous Wastes and Toxic Chemicals* (Environmental Protection Agency, Washington, D.C., to be published).